536114

ATOMIC DATA AND SPECTRAL LINE INTENSITIES FOR Ni XXI

A. K. Bhatia
NASA/Goddard Space Flight Center
Greenbelt, Maryland 20771 USA

and

E. Landi
Naval Research Laboratory
Washington DC 20375

ABSTRACT

Electron impact collision strengths, energy levels, oscillator strengths and spontaneous radiative decay rates are calculated for Ni XXI. The configurations used are $2s^22p^4$, $2s2p^5$, $2p^6$, $2s^22p^33s$, and $2s^23p^33d$ giving rise to 58 fine-structure levels in intermediate coupling. Collision strengths are calculated at five incident energies, 85, 170, 255, 340, and 425 Ry. Excitation rate coefficients are calculated by assuming a Maxwellian electron velocity distribution at an electron temperature of log $T_e(K)=6.9$, corresponding to maximum abundance of Ni XXI. Using the excitation rate coefficients and the radiative transition rates, statistical equilibrium equations for level populations are solved at electron densities 10^8-10^{14} cm^{-3}. Relative spectral line intensities are calculated. Proton excitation rates between the lowest three levels have been included in the statistical equilibrium equations. The predicted intensity ratios are compared with available observations.

CONTENTS

INTRODUCTION

Spectral lines from various elements in different stages of ionization have been observed in the Sun and other astrophysical objects and among these elements Ni ions are also present but with 18 times less abundance than the iron ions. The Ni XXI X-ray lines fall in a spectral range where a large number of lines from Fe also are observed, and since the latter dominate the spectrum, so far no identifications of X-ray Ni XXI lines have been made. At longer wavelengths only the forbidden transitions arising from the ground configuration $2s^22p^4$ have been identified in solar flares by Widing [1] and by Feldman et al. [2]. No trace is found in the literature of identifications of the resonance lines in the solar spectrum. These lines should be between 80 to 120 Å range due to transitions within the n=2 configurations.

Most of the observations of Ni XXI have been carried out in laboratory plasmas: Tokamak or laser-induced plasmas. X-ray lines have been observed by Swartz et al. [3] and Gordon et al. [4], while allowed transitions between the ground configuration and the first two excited configurations have been reported by a number of authors. Wavelength measurements are available from Lawson and Peakock [5] and Doschek et al. [6]. In the high-resolution spectra from the Princeton Large Torus (PLT) plasma, Ni XXI lines at 81.70, 88.72, 93.92, 95.86, 96.83, 100.24, 109.31, and 120.35 Å have been observed by Stratton et al. [7], Breton et al. [8], and Sugar et al. [9]. The lines in the wavelength range 80 to 340 Å in PLT plasma have been recorded by Dave et al. [10]. Among them are the Ni XXI lines at 95.86, 96.80, 97.15, 100.24, 109.31, and 120.35 Å. Forbidden transitions within the ground configuration levels have been observed in the laboratory by Doschek et al. [11], Hinnov et al. [12], Finkenthal et al. [13], and Hinnov et al. [14]. An up-to-date critical compilation of Ni XXI energy levels can be found in Shirai [15].

Accurate atomic data for this ion must be available for identification of various spectral lines and to infer properties of solar and astrophysical plasmas. The presently calculated data will be useful for any present and future observations.

In order to interpret data from space missions, atomic data such as energy levels, oscillator strengths, radiative transition rates, and collision strengths are required. Distorted wave calculations have been carried out for a number of ions such as Fe X [16], Fe XI [17], Fe XVII [18] and Fe XXI [19] in the past.

In this paper we carry out a distorted wave calculation for Ni XXI in the same way as for the Fe ions mentioned above. Since coupling between various channels is not included in the distorted wave approximation, the present calculation does not include resonances which could be important for forbidden transitions but usually not for dipole-allowed transitions for which most of the contribution to collision strengths comes from a very large number of incident partial waves.

We present energy levels, oscillator strengths, radiative transition rates, and collision strengths for Ni XXI for 58 fine-structure levels obtained by using the configurations $2s^22p^4$, $2s2p^5$, $2p^6$, $2s^22p^33s$, and $2s^22p^33d$ above the He-like core $1s^2$. These configurations give rise to 58 fine-structure levels in intermediate coupling.

We solve the statistical equilibrium equations for level populations at $\log T_e(K)=6.9$ where T_e is the temperature of maximum abundance of Ni XXI. For the known radiative transition rates the intensities of strong spectral lines can be calculated.

Atomic Data

The atomic data have been calculated using computer programs originally developed at University College London. These programs have been updated over the years. The energy levels, oscillator strengths, and radiative transition rates have been calculated by using the Superstructure program described by Eissner et al. [20]. The wavefunctions are of configuration interaction type and each configuration is expanded in terms of Slater orbitals. As indicated above, the configurations included are $2s^22p^4$, $2s2p^5$, $2p^6$, $2s^22p^33s$, and $2s^22p^33d$. The radial functions are calculated in a scaled Thomas-Fermi-Amaldi potential. The potential depends upon parameters λ_l which are determined variationally by optimizing the weighted sum of the term energies. They are found to be $\lambda_0 = 1.2850$, $\lambda_1 = 1.1837$, and $\lambda_2 = 1.0066$. The relativistic corrections are included by using Breit-Pauli Hamiltonian as a perturbation to the nonrelativistic Hamiltonian. Energy levels, oscillator strengths, and radiative transition rates are calculated in intermediate coupling.

The calculated energies for Ni XXI are listed in Table I. We use the calculated energy values to compute oscillator strengths and transition rates.

The scattering problem is carried out in the distorted wave approximation using programs described by Eissner and Seaton [21] and Eissner [22]. The reactance matrices are calculated in LS coupling. The collision strengths in intermediate coupling are calculated using these reactance matrices and the term-coupling coefficients obtained from structure calculations in the program JAJOM developed by Saraph [23] and modified recently by Saraph and Eissner [24]. The distorted wave calculations are carried out including intermediate angular momentum states L^T up to 33. The angular momentum L^T of the intermediate state is defined as

$$\vec{L^T} = \vec{l_i} + \vec{l_t} \tag{1}$$

where $\vec{l_i}$ is the angular momentum of the incident electron and $\vec{l_t}$ is the angular momentum of the target level. There is a considerable contribution to collision strengths from higher partial waves l_i, and we have added Coulomb-Bethe contributions for $l_i > 28$ to the dipole-allowed collision strengths. This contribution is calculated in the Coulomb-Bethe approximation using the program of Burgess and Sheorey [25]. The contributions from the higher partial waves to the non-dipole-allowed transitions have been added using the geometric progression. These additional contributions are referred to as top-up and this feature has recently been added to the program JAJOM [24].

The convergence of the collision strengths with respect to L^T has been demonstrated in most of the previous publications when the maximum L^T was 21. In the present case L^T is 33 and we expect all collision strengths to have converged. The Ni XXI collision strengths Ω_{ij}, the transition rates A_{ji}, and $g_i f_{ij}$, the absorption oscillator strengths multiplied by the statistical weight g_i of the lower level i are given in Table II.

The presently calculated wavelengths and gf values are compared in Table A for a few transitions with those obtained by Fawcett [25] by using five even-parity configurations $2s^2 2p^4$, $2p^6$, $2s^2 2p^3 3p$, $2s2p^4 3s$, and $2s2p^4 3d$ and six odd-parity configurations $2s2p^5$, $2s^2 2p^3 3s$, $2s^2 2p^3 3d$, $2s2p^4 3s$, $2s2p^4 3p$, and $2s2p^4 3d$, The agreement is fairly good especially for the transitions within the low-lying levels.

The convergence of collision strengths with respect to L^T for the highest energy 425 Ry is shown in Table B for a set of randomly chosen transitions. The convergence is good and addition of more incident partial waves will not improve the results. It is expected that collision strengths at lower energies must have converged.

Line Emissivity

The number of photons observed in optically thin spectral line $j \to i$ is given by

$$I_{ij} = \frac{1}{4\pi} \int_h N_j(X^{+m}) A_{ji} dh \qquad ph\ cm^{-2}\ s^{-1}\ sr^{-1} \tag{2}$$

If the *Contribution Function* $G_{ij}(T, N_e)$ of the line is defined as

$$G(T, \lambda_{i,j}) = \frac{N_j(X^{+m})}{N(X^{+m})} \frac{N(X^{+m})}{N(X)} \frac{N(X)}{N(H)} \frac{N(H)}{N_e} \frac{A_{ji}}{N_e} \tag{3}$$

where

1. - $\frac{N_j(X^{+m})}{N(X^{+m})}$ is the relative upper level population;

2. – $\frac{N(X^{+m})}{N(X)}$ is the relative abundance of the ion X^{+m} (*ion fraction*); this quantity is taken from the literature under the assumption of ionization equilibrium;

3. – $\frac{N(X)}{N(H)}$ is the abundance of the element X relative to hydrogen;

4. – $\frac{N(H)}{N_e}$ is the hydrogen abundance relative to the electron density (≈ 0.8 for fully ionized plasmas);

5. – A_{ji} is the Einstein coefficient for spontaneous emission.

and the *Differential Emission Measure* (DEM) is introduced as

$$\varphi(T) = N_e^2 \frac{dh}{dT} \tag{4}$$

the number of photons emitted in a spectral line may be expressed as

$$I_{ij} = \frac{1}{4\pi} \times \int_T G(T, \lambda_{i,j}) \varphi(T) dT \tag{5}$$

In the present work, we are interested in evaluating the $G_{ij}(T, N_e)$ function for all the Ni XXI lines.

The relative population $\frac{N_j(X^{+m})}{N(X^{+m})}$ must be calculated by solving the statistical equilibrium equations for a number of low lying levels and including all the important collisional and radiative excitation and de-excitation mechanisms:

$$\begin{aligned} N_j (N_e \Sigma_i C^e_{j,i} + N_p \Sigma_i C^p_{j,i} + \Sigma_{i>j} R_{j,i} + \Sigma_{i<j} A_{j,i}) = \\ \Sigma_i N_i (N_e C^e_{i,j} + N_p C^p_{i,j}) + \Sigma_{i>j} N_i A_{i,j} + \Sigma_{i<j} N_i R_{i,j} \end{aligned} \tag{6}$$

with $C^e_{j,i}$ and $C^p_{j,i}$ the electron and proton collisional excitation rate coefficients (cm^3 sec^{-1}), $R_{j,i}$ the stimulated absorption rate coefficient (sec^{-1}) and $A_{j,i}$ the spontaneous radiation transition probability (sec^{-1}). In typical solar conditions it is possible to neglect the stimulated absorption and emission mechanisms. However, since Ni XXI is formed at very high temperature, proton rates may give a significant contribution to the population of excited levels, and so they cannot be neglected.

Collisional Data Fitting Technique

The electron excitation coefficient $C^e_{i,j}$ is given by

$$C^e_{i,j} = \frac{8.63 \times 10^{-6}}{T_e^{1/2}} \frac{\Upsilon_{i,j}(T_e)}{g_i} \; exp\left(-\frac{E_{i,j}}{kT_e}\right) \tag{7}$$

where g_i is the statistical weight of level i; $E_{i,j}$ is the energy difference between levels i and j; k is the Boltzmann constant and $\Upsilon_{i,j}$ is the thermally-averaged collision strength:

$$\Upsilon_{i,j}(T_e) = \int_0^\infty \Omega_{i,j} \; exp\left(-\frac{E_j}{kT_e}\right) d\left(\frac{E_j}{kT_e}\right) \tag{8}$$

where E_j is the energy of the scattered electron relative to the final energy state of the ion, and Ω_{ij} is the collision strength for the transition.

In order to carry out the integration in Equation (7), it is necessary to know the collision strength Ω across the whole energy range, from threshold to infinity. However, theoretical calculations only provide the collision strength for a limited number of energy values (i.e. in the case of the present Ni XXI calculation, only five energy values are provided), so that some interpolation/extrapolation technique is required in order to properly take into account the energy dependence of the collision strength.

In the present work we have adopted the method described by Burgess and Tully [27] to extrapolate the collision strengths to the high- and low-energy limit. This method consists of scaling both the electron energy and the collision strengths according to the transition types: allowed, forbidden and intercombination transitions. Different scaling laws have been developed in order to better reproduce the behaviour of the collision strengths according to each type of transition. The scaling laws are:

$$E_{scal} = 1 - \frac{\ln C_\Omega}{\ln\left(\frac{E}{E_{ij}} + C_\Omega\right)} \qquad \Omega_{scal} = \frac{\Omega}{\ln\left(\frac{E}{E_{ij}} + e\right)} \tag{9}$$

for the allowed transitions,

$$E_{scal} = \frac{\frac{E}{E_{ij}}}{\frac{E}{E_{ij}} + C_\Omega} \qquad \Omega_{scal} = \Omega \tag{10}$$

for the forbidden transitions, and

$$E_{scal} = \frac{\frac{E}{E_{ij}}}{\frac{E}{E_{ij}} + C_\Omega} \qquad \Omega_{scal} = \left(\frac{E}{E_{ij}} + 1\right)^2 \Omega \tag{11}$$

for the intercombination transitions. The constant C_Ω is chosen to optimize the fit of the calculated data.

In the case of the allowed transitions, the Ω value at $E \to \infty$ ($E_{scal} = 1$) is set to be the transition's oscillator strengths, according to the Coulomb-Bethe approximation. The collision strengths are then interpolated for intermediate values of E_{scal}, and extrapolated to $E_{scal} = 0$ and $E_{scal} = 1$ (corresponding to E=0 and E$\to \infty$); the interpolated/extrapolated values are used to calculate the effective collision strength according to Equation (8). This scaling has two main advantages:

1. Allows to calculate the effective collision strengths more accurately by better sampling the energy dependence of the collision strength;

2. Allows to take into account the high-energy behaviour of the collision strength.

The high energy behavior of the collision strength is of particular importance for the allowed transitions, as its contribution to the calculation of the effective collision strength can be very important. The use of the Coulomb-Bethe approximation allows us to use the oscillator strength of the transition both as a high-energy point for the interpolation and integration procedures, and to have an independent check on the quality of the calculation of the collision strength itself.

Examples of the present scaling to type 1, 2, and 3 is shown in Figures 1,2, and 3, respectively.

Results

The atomic data and transition probabilities calculated in the present work and given Tables I and II have been used to solve the statistical equilibrium equations (6); the proton excitation rates given by Ryans et al. [28] have been also used. The proton rate coefficients at log T_e(K)=6.9 are 1.36×10^{-11}, 1.19×10^{-11}, and 1.22×10^{-11} cm^3/s for the transitions $1 \to 2$, $1 \to 3$, and $2 \to 3$, respectively. The ion fraction (0.16) of Mazzotta [29] and the element abundance (6.92×10^{-6}) of Feldman [30] for Ni have been also used.

Table IIIA and IIIB show the fractional level population $\frac{N_i(X^{+m})}{N(X^{+m})}$ for all the levels in the Ni XXI atomic model, calculated without and with the proton excitation rates, respectively, at $log(N_e(cm^{-3}))$=8, 9, 10, 11, 12, 13, and 14. The differences between the two computations are significant, but limited to a maximum of 20% in the worst cases. The only levels having a significant population belong to the ground configuration. However, at high density, a few more metastable levels reach a significant population, these being the levels with $j = 4, 5$, their radiative decay is given only by intercombination or forbidden transitions with small Einstein coefficients A_{ji}.

Tables IVA and IVB list the relative line emissivities (the absolute emissivities can be obtained by multiplying the relative emissivities by the appropriate factors given earlier) for the strongest lines emitted by Ni XXI, calculated again without and with the proton excitation rates. It is possible to see that there are three different wavelength ranges where Ni XXI lines are strongest: the X-rays lines at around 11 Å, where n=3 to n=2 transitions are found; the Extreme Ultraviolet (EUV) lines between 80 and 140 Å, where the allowed n=2 to n=2 transitions are emitted; and the EUV and Ultraviolet lines between 350 and 3000 Å, given by the forbidden transitions within the ground configurations.

Diagnostic Potential

Ni XXI predicted emissivities do not show a marked density sensitivity in nearly all cases. Their use for density diagnostics is therefore limited. In the X-ray wavelength range only the $2s2p^3(^2P)3d\ ^3P_1 \to 2s^22p^4\ ^3P_2$ transition is density sensitive in the range 9.0<log(N_e) <10.0 and can potentially provide reliable density measurements. The relatively strong n=2 to n=2 allowed transitions, observable between 80 and 130 Å, are only weakly density sensitive relative to each other, so no use can be made of these lines for density diagnostics. The forbidden transitions at 1077.47 Å within the ground configurations ($^3P_0 \to {}^3P_2$ levels) provide a potentially useful density diagnostics. However, the intensity of this line is predicted to decrease as density increases, with the result that it is very difficult to observe this transition.

If observed simultaneously, line ratios involving one of the n=2 to n=2 allowed lines (wavelengths between 80 and 130 Å) and one from the n=3 to n=2 transitions (wavelengths shorter than 15 Å) can provide excellent temperature diagnostics. This is due to the strong temperature dependence of the excitation rates for the n=3 levels.

The mild density sensitivity of the Ni XXI lines can provide excellent tools for Differential Emission Measure studies (Mason and Monsignori Fossi [31]).

Comparison With Observations

In order to test the accuracy of the present theoretical calculations, we have compared predicted line intensities with the observed values of Stratton et al. [7], who provide line intensities for $n = 2$ to $n = 2$ transitions relative to the $2s2p^5\ ^3P_2 \to 2s^22p^4\ ^3P_2$ transition at 95.85 Å. Table C presents the comparison between the measured and predicted intensity ratios for a number of lines. This table shows that the branching ratio 109.31/95.86 is in excellent agreement with its predicted value, given by the ratio of the spontaneous radiative transition probabilities, the upper level being the same for the two transitions. The branching ratio 120.35/95.86 is higher than predicted, thus suggesting the presence of an unidentified line blending the 120.35 Å transition. It is important to note that the 120.35/95.86 ratio has not been reported by Stratton et al. [7] and has been determined directly from the spectra given in that paper, so that its accuracy should be taken with caution. Good agreement between theory and observation is also found for the 88.82/95.86 ratio, while the predicted intensity of the 93.92 Å line confirms that this line is rather weak, consistent with the absence of this ratio in the measurements of Stratton et al. [7]. The 96.83/95.86 observed ratio is higher than predicted, probably due to an unresolved blending line: it is to be noted that the branching ratio 88.82/96.83 also does not agree with the observations.

This data set has been made available in the CHIANTI database [32]. We hope the data presented in this paper will be useful to analyze observations of Ni XXI lines from the Sun and other astrophysical objects.

Acknowledgment

This work was supported by NASA grant from the Applied Information Systems Research Program under Contract W19,539. The work of Enrico Landi is supported by the Office of Naval Research. Calculations were carried out using Cray Y-MP computer of the NASA Center for Computation Science.

References

1. K. G. Widing, Astrophys. J. **222**, 735 (1978)
2. U. Feldman, W. Curdt, E. Landi, and K. Wilhelm, Astrophys. J. **544**, 508 (200)
3. M. Swartz, S. O. Kastner, E. Rothe, and W. Neupert, J.Phys.B **4**, 1747 (1971)
4. H. Gordon, M. G. Hobby, and N. J. Peacock, J.Phys.B **13**, 1985 (1980)
5. K. D. Lawson, and N. J. Peacock, J.Phys. B **13**, 3313 (1980)
6. G. A. Doschek, U. Feldman, J. Davis, and R. D. Cowan, Phys.Rev.A **12** , 980 (1975)
7. B. C. Stratton, H. W. Moos, S. Suckewer, U. Feldman, J. F. Seely, and A. K. Bhatia, Phys. Rev. **31**, 2534 (1985)
8. C. Breton, C. De Michelis, M. Finkenthal, and M. Mattioli, J.Opt.Soc.Am. **69**, 1652 (1979)
9. J. Sugar, V. Kaufman, and W. L. Rowan, J.Opt.Soc.Am. B **9**, 344 (1992)
10. J. H. Dave, U. Feldman, J. F. Seely, A. Wouters, S. Suckewer, E. Hinnov, and J. L. Schwob, J. Opt. Soc. Am. B **4**, 635 (1987)
11. G. A. Doschek, U. Feldman, R. D. Cowan, and L. Cohen, Astrophys. J. **188**, 417 (1974)
12. E. Hinnov, S. Suckewer, S. Cohen, and K. Sato, Phys.Rev.A **25**, 2293 (1982)
13. M. Finkenthal, R. E. Bell, H. W. Moos, and TFR group, J.Appl.Phys. **56**, 2012 (1984)
14. E. Hinnov, B. Denne, A. Ramsey, B. Stratton, and J. Timberlake, J.Opt.Soc.Am. B **7**, 2002 (1990)
15. T. Shirai, J. Sugar, A. Musgrove, and W. L. Wiese, J.Phys.Chem.Ref.Data, Monograph 8 (2000)
16. A. K. Bhatia and G. A. Doschek, ATOMIC DATA AND NUCLEAR DATA TABLES **60**, 97 (1995)
17. A. K. Bhatia and G. A. Doschek, ATOMIC DATA AND NUCLEAR DATA TABLES **64**, 183 (1996)
18. A. K. Bhatia and G. A. Doschek, ATOMIC DATA AND NUCLEAR DATA TABLES **52**, 1 (1992)
19. K. J. H. Phillips, A. K. Bhatia, H. E. Mason, and D. M. Zarro, Astrophys. J. **466**, 549 (1996)
20. W. Eissner, M. Jones, and H. Nussbaumer, Comput. Phys. Commun. **8**, 270 (1972)
21. W. Eissner and M. J. Seaton, J. Phys. B **5**, 2187 (1979)
22. W. Eissner, Comput. Phys. Commun. **114**, 295 (1998)
23. H. E. Saraph, Comput. Phys. Commun. **15**, 247 (1978)
24. H. E. Saraph and W. Eissner, Comput. Phys. Commun. (to be published)

25. A. Burgess and V. B. Sheorey, J. Phys. B **7**, 2403 (1974)

26. B. C. Fawcett, ATOMIC DATA AND NUCLEAR DATA TABLES **34**, 215 (1986)

27. A. Burgess, J. A. Tully, Astron. and Astrophys. **254**, 436 (1992)

28. R. S. I. Ryans, F. P. Keenan, R. H. G. Reid, ATOMIC DATA AND NUCLEAR DATA TABLES, (in preparation), (2001)

29. P. Mazzotta, G. Mazzitelli, S. Colafrancesco, and N. Vittorio, Astron. and Astrophys. **133**, 403 (1998)

30. U. Feldman, Phys. Scr.**46**, 202 (1992)

31. H. E. Mason and B. C. Monsignori Fossi, Astron. Astroph. Review **6**, 123 (1994)

32. K. P. Dere, H. E. Mason, B. C. Monsignori Fossi, and P. R. Young, Astron.Astroph. Suppl. **125**, 149 (1997)

Table I. Calculated Energy Levels for Ni XXI

Key	A number assigned to each level
Configuration	The configuration with $1s^2 2s^2 2p^4$ truncated
Level	The term designation of the level within the configuration
Energy	calculated level energies in units of cm^{-1}

Table II. Ni XXI Oscillator Stengths, Radiative Decay Rates, and Collision Strengths

Lower and Upper Level	The lower and upper levels, where the numbers refer to the Key listed in Table I
Oscillator Strength	gf, the (dimensionless) product of the statistical weight g of the lower level and the absorption oscillator strength f
Radiative Decay Rate	The spontaneous radiative decay rate A_{ji} in units of s^{-1}
Collision Strength	The dimensionless electron impact collision strength Ω at the energy (in units of Ry) given in the table heading

Table IIIA. Ni XXI Fractional Level Populations: Without Proton Excitation
Table IIIB. Ni XXI Fractional Level Populations: With Proton Excitation

Den.	The electron density in cm^{-3} (log scale)
Key	A number assigned to each level as given in Table I
Population	The fractional level populations n_j as a function of electron density for an electron temperature log T_e(K)=6.9: the sum of all fractional level populations is defined as unity

Table IVA. Ni XXI Line Intensities: Without Proton Excitation
Table IVB. Ni XXI Line Intensities: With Proton Excitation

Den.	The electron density in cm^{-3} (log scale)
j and i	The upper and lower levels, where the numbers refer to the Key listed in Table I
Wavelength	The wavelengths in units of Å
Intensity	The relative intensity ($n_j A_{ji}$ in units of photon/sec) for the indicated density given in the table heading and for an electron temperature of log T_e(K)=6.9

Table A. Comparison of the presently calculated gf values with those of Fawcett [26]

Transition		Fawcett		Present	
i	j	λ	gf	λ	gf
1	6	95.898	0.292	95.39	0.301
1	7	88.864	0.140	88.37	0.141
1	9	69.661	0.036	68.81	0.35
1	11	12.811	0.025	12.50	0.021
1	12	12.731	0.228	12.41	0.177
2	7	96.696	0.076	96.15	0.076
2	12	12.881	0.053	12.56	0.041
3	6	109.274	0.098	108.77	0.099
3	7	100.234	0.061	99.74	0.062
3	8	93.971	0.091	93.47	0.092
3	12	12.942	0.048	12.62	0.035
3	13	12.729	0.034	12.42	0.034
4	6	120.288	0.035	120.13	0.033
4	9	81.693	0.479	80.82	0.498
5	9	97.183	0.052	95.40	0.048

Table B. Convergence of Collision Strength with L^T for k^2=425 Ry

Transition		L^T				
i	j	17	21	25	29	33
1	2	8.762-03	9.455-03	9.519-03	9.541-03	9.555-03
1	3	1.614-02	1.580-02	1.597-02	1.601-02	1.603-02
1	4	1.549-02	1.396-02	1.404-02	1.406-02	1.409-02
1	6	7.669-01	7.667-01	7.666-01	7.666-01	7.667-01
1	7	3.254-01	3.253-01	3.252-01	3.253-01	3.254-01
1	28	9.274-02	1.045-01	1.095-01	1.117-01	1.126-01
1	43	1.364-01	1.624-01	1.735-01	1.782-01	1.802-01
2	7	1.964-01	1.964-01	1.963-01	1.963-01	1.962-01
3	6	3.028-01	3.029-01	3.029-01	3.029-01	3.028-01
3	7	1.678-01	1.678-01	1.678-01	1.678-01	1.678-01
3	8	2.303-01	2.302-01	2.302-01	2.303-01	2.303-01
3	38	9.332-02	1.077-01	1.138-01	1.165-01	1.176-01
4	56	3.568-01	3.662-01	3.707-01	3.726-01	3.735-01
5	58	1.738-01	1.764-01	1.776-01	1.781-01	1.783-01
9	10	7.890-01	7.892-01	7.894-01	7.896-01	7.897-01
11	21	2.132-01	1.503-01	1.469-01	1.479-01	1.490-01
11	22	1.406-01	1.055-01	1.038-01	1.045-01	1.053-01
18	48	1.757-01	1.380-01	1.354-01	1.364-01	1.374-01
53	55	1.049-01	9.932-02	9.908-02	9.961-02	1.001-01
56	57	1.128-01	1.077-01	1.077-01	1.082-01	1.087-01

Table C. Comparison between observed intensity ratios and predicted values [a].

Transition	λ (Å)	I_{obs}	I_{pred}
$2s2p^{51}P_1 \rightarrow 2s^22p^{41}D_2$	81.70	blend	0.170
$2s2p^{53}P_1 \rightarrow 2s^22p^{43}P_2$	88.82	0.33	0.390
$2s2p^{53}P_0 \rightarrow 2s^22p^{43}P_1$	93.92	0.00	0.050
$2s2p^{53}P_2 \rightarrow 2s^22p^{43}P_2$	95.86	1.00	1.000
$2s2p^{53}P_1 \rightarrow 2s^22p^{43}P_0$	96.83	0.27	0.180
$2s2p^{53}P_1 \rightarrow 2s^22p^{43}P_1$	100.24	blend	0.135
$2s2p^{53}P_2 \rightarrow 2s^22p^{43}P_21$	109.31	0.25	0.252
$2s2p^{53}P_2 \rightarrow 2s^22p^{41}D_2$	120.35	0.18	0.068

[a]Comparison between observed intensity ratios from Stratton et al. [7] and the predicted values. The $2s2p^5$ $^3P_2 \rightarrow 2s^22p^4$ $^3P_2$ line at 95.86 Å has been taken as the reference line. The $2s2p^5$ $^3P_2 \rightarrow 2s^22p^4$ $^1D_2$ ratio is not listed in Stratton et al. [7] and has been measured from the spectra presented in their paper.

Table I. Calculated Energy Levels for Ni XXI

Key	Configuration	Level	Energy
1	$2s^2 2p^4$	$^3P_2$	0.
2		$^3P_0$	91559.
3		$^3P_1$	129003.
4		$^1D_2$	215946.
5		$^1S_0$	405045.
6	$2s2p^5$	$^3P_2$	1048380.
7		$^3P_1$	1131633.
8		$^3P_0$	1198892.
9		$^1P_1$	1453228.
10	$2p^6$	$^1S_0$	2445574.
11	$2s^2 2p^3 3s$	$^5S_2$	8001925.
12		$^3S_1$	8054803.
13		$^3D_2$	8177583.
14		$^3D_1$	8181637.
15		$^3D_3$	8220180.
16		$^1D_2$	8241451.
17		$^3P_0$	8335736.
18		$^3P_1$	8344240.
19		$^3P_2$	8426443.
20		$^1P_1$	8443478.
21	$2s^2 2p^3 3d$	$^5D_3$	8616343.
22		$^5D_2$	8616412.
23		$^5D_0$	8617210.
24		$^5D_1$	8617665.
25		$^5D_4$	8622341.
26		$^3D_2$	8666142.
27		$^3D_1$	8702146.
28		$^3D_3$	8702315.
29		$^3F_2$	8782232.
30		$^3F_3$	8793696.
31		$^1S_0$	8795345.
32		$^3G_3$	8795558.
33		$^1G_4$	8798489.
34		$^3D_1$	8799598.
35		$^3F_4$	8830218.
36		$^3G_4$	8841095.
37		$^3G_5$	8841819.
38		$^3D_2$	8851440.
39		$^3P_1$	8855574.
40		$^3D_3$	8873795.
41		$^3P_0$	8876006.
42		$^1P_1$	8883411.

Table I. Calculated Energy Levels for Ni XXI

Key	Configuration	Level	Energy
43		$^3P_2$	8884630.
44		$^3F_2$	8903300.
45		$^3S_1$	8907361.
46		$^1F_3$	8932869.
47		$^1D_2$	8963642.
48		$^3D_3$	8977444.
49		$^1D_2$	8989679.
50		$^3P_1$	9015923.
51		$^3F_4$	9037889.
52		$^3P_0$	9045878.
53		$^3P_2$	9054369.
54		$^3D_1$	9059752.
55		$^3F_3$	9078661.
56		$^1F_3$	9097701.
57		$^3D_2$	9101010.
58		$^1P_1$	9169597.

Table II. Ni XXI Oscillator Strengths, Radiative Decay Rates, and Collision Strengths

Low. Lev.	Upp. Lev.	Osc. Str.	Rad. Dec. Rate	Collision Strength Impact Electron Energy (Ry)				
i	j	gf	(1/s)	85	170	255	340	425
1	2		9.718-01	9.964-03	9.343-03	9.320-03	9.423-03	9.555-03
	3		4.245+04	2.377-02	1.893-02	1.710-02	1.631-02	1.603-02
	4		4.309+04	2.640-02	1.905-02	1.614-02	1.478-02	1.409-02
	5		9.437+00	9.286-04	4.622-04	2.806-04	1.969-04	1.576-04
	6	3.005-01	4.406+10	5.461-01	6.330-01	6.906-01	7.331-01	7.667-01
	7	1.412-01	4.020+10	2.302-01	2.675-01	2.924-01	3.108-01	3.254-01
	8			1.333-04	7.576-05	4.873-05	3.413-05	2.539-05
	9	3.509-02	1.648+10	4.276-02	4.852-02	5.265-02	5.584-02	5.841-02
	10		7.735+04	1.247-04	9.049-05	7.798-05	7.230-05	6.932-05
	11	2.009-02	1.716+11	2.327-03	1.524-03	1.364-03	1.384-03	1.462-03
	12	1.772-01	2.557+12	2.220-03	4.830-03	7.225-03	9.217-03	1.090-02
	13	1.249-01	1.114+12	1.892-03	3.456-03	4.985-03	6.281-03	7.384-03
	14	2.271-03	3.380+10	7.077-04	3.909-04	2.904-04	2.604-04	2.567-04
	15	2.025-01	1.304+12	2.676-03	5.476-03	8.075-03	1.026-02	1.211-02
	16	1.925-02	1.744+11	1.264-03	1.004-03	1.056-03	1.180-03	1.317-03
	17			1.936-05	8.883-06	4.941-06	3.110-06	2.130-06
	18	6.018-03	9.315+10	8.694-05	1.609-04	2.421-04	3.171-04	3.840-04
	19	1.717-02	1.626+11	2.664-04	4.529-04	6.722-04	8.737-04	1.052-03
	20	2.836-03	4.495+10	1.505-04	1.188-04	1.285-04	1.467-04	1.659-04
	21	1.483-02	1.049+11	1.110-02	4.844-03	3.317-03	2.825-03	2.659-03
	22	4.520-02	4.477+11	8.272-03	4.991-03	4.553-03	4.649-03	4.875-03
	23			1.086-03	3.575-04	1.666-04	9.376-05	5.936-05
	24	3.105-02	5.126+11	4.398-03	2.781-03	2.649-03	2.782-03	2.969-03
	25			1.351-02	4.916-03	2.589-03	1.690-03	1.258-03
	26	2.858-01	2.864+12	1.606-02	1.865-02	2.215-02	2.521-02	2.781-02
	27	2.063-02	3.474+11	3.667-03	3.616-03	3.998-03	4.338-03	4.619-03
	28	1.287+00	9.287+12	4.358-02	6.769-02	8.618-02	1.007-01	1.126-01
	29	1.879-01	1.933+12	8.276-03	1.035-02	1.262-02	1.457-02	1.621-02
	30	4.862-01	3.583+12	1.866-02	2.544-02	3.170-02	3.688-02	4.119-02
	31			1.025-03	3.642-04	1.777-04	1.032-04	6.678-05
	32	9.870-02	7.276+11	7.026-03	6.690-03	7.553-03	8.482-03	9.313-03
	33			5.512-03	3.682-03	3.463-03	3.466-03	3.518-03
	34	9.162-02	1.577+12	5.452-03	5.832-03	6.797-03	7.696-03	8.477-03
	35			4.439-03	1.798-03	1.178-03	9.895-04	9.082-04
	36			5.418-03	1.903-03	9.647-04	6.097-04	4.418-04
	37			6.030-03	4.702-03	4.696-03	4.823-03	4.946-03
	38	4.830-01	5.048+12	1.784-02	2.581-02	3.269-02	3.842-02	4.325-02
	39	1.795-01	3.130+12	6.467-03	9.261-03	1.173-02	1.376-02	1.548-02
	40	3.448+00	2.587+13	9.803-02	1.674-01	2.172-01	2.559-01	2.873-01
	41			8.080-04	2.755-04	1.316-04	7.544-05	4.841-05
	42	2.085-01	3.658+12	8.556-03	1.134-02	1.399-02	1.621-02	1.808-02
	43	2.153+00	2.267+13	6.270-02	1.060-01	1.369-01	1.608-01	1.802-01
	44	1.390-04	1.470+09	3.875-03	1.410-03	7.402-04	4.983-04	3.939-04
	45	1.088+00	1.919+13	3.311-02	5.385-02	6.923-02	8.126-02	9.113-02
	46	8.202-01	6.236+12	2.512-02	4.029-02	5.180-02	6.083-02	6.819-02
	47	4.955-04	5.311+09	4.471-04	2.162-04	1.880-04	1.904-04	2.040-04

TABLE IIIA. Ni XXI Fractional Level Populations: Without Proton Excitation

log(Den.)	8	9	10	11	12	13	14
Key				Population			
1	9.956-01	9.670-01	9.082-01	8.880-01	8.825-01	8.545-01	6.982-01
2	4.448-03	3.295-02	9.174-02	1.116-01	1.139-01	1.125-01	1.024-01
3	2.356-07	2.354-06	2.349-05	2.345-04	2.324-03	2.138-02	1.171-01
4	1.228-07	1.220-06	1.203-05	1.197-04	1.191-03	1.139-02	7.993-02
5	1.050-09	1.081-08	1.147-07	1.170-06	1.183-05	1.280-04	1.784-03
6	4.058-13	3.945-12	3.713-11	3.633-10	3.618-09	3.563-08	3.237-07
7	1.350-13	1.426-12	1.584-11	1.638-10	1.642-09	1.622-08	1.489-07
8	1.146-16	1.233-15	1.441-14	1.845-13	5.275-12	3.648-10	1.936-08
9	9.356-15	9.292-14	9.160-13	9.129-12	9.261-11	1.057-09	1.966-08
10	2.873-17	3.063-16	3.453-15	3.586-14	3.611-13	3.695-12	4.279-11
11	3.058-16	3.038-15	2.997-14	2.982-13	2.974-12	2.908-11	2.525-10
12	1.331-17	1.335-16	1.345-15	1.348-14	1.345-13	1.315-12	1.136-11
13	2.952-17	2.892-16	2.769-15	2.727-14	2.720-13	2.697-12	2.558-11
14	4.186-18	4.315-17	4.581-16	4.675-15	4.728-14	5.105-13	6.978-12
15	8.371-17	8.133-16	7.642-15	7.474-14	7.441-13	7.330-12	6.778-11
16	1.553-17	1.509-16	1.419-15	1.388-14	1.387-13	1.410-12	1.578-11
17	1.785-19	3.844-18	8.092-17	9.550-16	9.915-15	1.163-13	2.040-12
18	1.052-18	2.235-17	4.677-16	5.505-15	5.621-14	5.752-13	6.427-12
19	2.828-18	2.798-17	2.737-16	2.723-15	2.782-14	3.355-13	6.523-12
20	6.362-19	6.623-18	7.163-17	7.358-16	7.512-15	8.749-14	1.662-12
21	8.800-16	8.679-15	8.430-14	8.344-13	8.313-12	8.129-11	7.058-10
22	1.635-16	1.616-15	1.578-14	1.565-13	1.560-12	1.528-11	1.340-10
23	4.667-17	4.888-16	5.343-15	5.497-14	5.510-13	5.458-12	5.090-11
24	7.003-17	7.107-16	7.321-15	7.392-14	7.386-13	7.245-12	6.401-11
25	1.362-10	1.351-09	1.328-08	1.320-07	1.316-06	1.286-05	1.110-04
26	5.051-17	4.954-16	4.751-15	4.682-14	4.665-13	4.585-12	4.103-11
27	5.628-18	8.765-17	1.524-15	1.743-14	1.770-13	1.768-12	1.720-11
28	7.559-17	7.366-16	6.966-15	6.829-14	6.790-13	6.589-12	5.461-11
29	4.847-17	4.733-16	4.498-15	4.417-14	4.402-13	4.351-12	4.048-11
30	6.934-17	6.763-16	6.412-15	6.291-14	6.259-13	6.104-12	5.244-11
31	7.168-17	7.170-16	7.174-15	7.176-14	7.185-13	7.257-12	7.530-11
32	1.047-16	1.023-15	9.736-15	9.567-14	9.537-13	9.444-12	8.910-11
33	4.301-11	4.248-10	4.139-09	4.102-08	4.098-07	4.099-06	4.076-05
34	9.706-18	1.186-16	1.629-15	1.779-14	1.795-13	1.774-12	1.640-11
35	1.473-11	1.437-10	1.365-09	1.340-08	1.338-07	1.353-06	1.478-05
36	1.896-10	1.842-09	1.730-08	1.692-07	1.688-06	1.691-05	1.740-04
37	3.422-10	3.324-09	3.122-08	3.053-07	3.041-06	3.011-05	2.873-04
38	1.406-17	1.369-16	1.293-15	1.267-14	1.273-13	1.353-12	1.735-11
39	9.779-18	1.059-16	1.226-15	1.283-14	1.290-13	1.290-12	1.281-11
40	6.250-17	6.072-16	5.704-15	5.578-14	5.544-13	5.375-12	4.433-11
41	5.986-19	5.889-18	5.692-17	5.658-16	5.986-15	9.056-14	2.452-12
42	6.960-18	7.035-17	7.190-16	7.247-15	7.302-14	7.738-13	9.862-12
43	4.255-17	4.134-16	3.886-15	3.801-14	3.779-13	3.675-12	3.087-11
44	2.708-18	2.719-17	2.742-16	2.757-15	2.832-14	3.528-13	7.785-12
45	1.971-17	1.914-16	1.798-15	1.758-14	1.749-13	1.707-12	1.480-11
46	2.027-17	1.970-16	1.852-15	1.812-14	1.806-13	1.801-12	1.828-11

TABLE IIIA. Ni XXI Fractional Level Populations: Without Proton Excitation

log(Den.)	8	9	10	11	12	13	14
Key				Population			
47	9.451-19	1.407-17	2.361-16	2.692-15	2.815-14	3.591-13	8.225-12
48	7.354-18	8.050-17	9.488-16	9.982-15	1.011-13	1.074-12	1.493-11
49	2.861-18	2.945-17	3.121-16	3.191-15	3.308-14	4.315-13	9.593-12
50	7.207-19	4.210-17	1.141-15	1.385-14	1.413-13	1.402-12	1.312-11
51	1.249-12	1.261-11	1.286-10	1.298-09	1.329-08	1.615-07	3.268-06
52	3.727-20	4.057-19	4.764-18	5.316-17	8.552-16	3.781-14	1.855-12
53	1.128-17	1.102-16	1.047-15	1.030-14	1.039-13	1.141-12	1.667-11
54	3.257-19	4.510-18	7.100-17	8.057-16	8.975-15	1.638-13	5.392-12
55	5.858-17	5.698-16	5.369-15	5.257-14	5.234-13	5.148-12	4.686-11
56	4.178-19	4.244-18	4.386-17	4.501-16	5.187-15	1.166-13	5.499-12
57	5.842-19	5.770-18	5.629-17	5.665-16	6.521-15	1.451-13	5.962-12
58	6.518-20	7.015-19	8.046-18	8.457-17	9.141-16	1.530-14	6.264-13

TABLE IIIB. Ni XXI Fractional Level Populations: With Proton Excitation

log(Den.)	8	9	10	11	12	13	14
Key				Population			
1	9.967-01	9.751-01	9.293-01	9.131-01	9.082-01	8.810-01	7.256-01
2	3.335-03	2.493-02	7.070-02	8.659-02	8.848-02	8.778-02	8.208-02
3	2.130-07	2.133-06	2.139-05	2.140-04	2.122-03	1.959-02	1.095-01
4	1.229-07	1.223-06	1.209-05	1.204-04	1.198-03	1.146-02	8.038-02
5	1.049-09	1.072-08	1.123-07	1.142-06	1.155-05	1.251-04	1.757-03
6	4.062-13	3.977-12	3.796-11	3.732-10	3.719-09	3.663-08	3.326-07
7	1.347-13	1.405-12	1.528-11	1.570-10	1.574-09	1.556-08	1.435-07
8	1.142-16	1.209-15	1.375-14	1.738-13	4.870-12	3.350-10	1.812-08
9	9.359-15	9.310-14	9.208-13	9.186-12	9.321-11	1.065-09	1.982-08
10	2.866-17	3.009-16	3.313-15	3.420-14	3.442-13	3.531-12	4.147-11
11	3.059-16	3.044-15	3.012-14	3.000-13	2.992-12	2.928-11	2.552-10
12	1.330-17	1.334-16	1.342-15	1.344-14	1.341-13	1.312-12	1.139-11
13	2.954-17	2.909-16	2.813-15	2.780-14	2.773-13	2.750-12	2.603-11
14	4.181-18	4.279-17	4.486-16	4.562-15	4.609-14	4.957-13	6.732-12
15	8.380-17	8.200-16	7.818-15	7.684-14	7.655-13	7.548-12	6.994-11
16	1.555-17	1.522-16	1.451-15	1.427-14	1.426-13	1.449-12	1.613-11
17	1.705-19	3.265-18	6.572-17	7.739-16	8.059-15	9.696-14	1.830-12
18	1.005-18	1.902-17	3.803-16	4.465-15	4.563-14	4.716-13	5.542-12
19	2.829-18	2.807-17	2.759-16	2.749-15	2.805-14	3.343-13	6.383-12
20	6.352-19	6.550-18	6.970-17	7.128-16	7.274-15	8.480-14	1.626-12
21	8.805-16	8.713-15	8.519-14	8.450-13	8.422-12	8.243-11	7.180-10
22	1.635-16	1.621-15	1.592-14	1.581-13	1.577-12	1.546-11	1.359-10
23	4.658-17	4.826-16	5.180-15	5.303-14	5.313-13	5.266-12	4.928-11
24	6.999-17	7.078-16	7.244-15	7.301-14	7.294-13	7.161-12	6.349-11
25	1.362-10	1.354-09	1.336-08	1.330-07	1.326-06	1.297-05	1.124-04
26	5.055-17	4.981-16	4.824-15	4.768-14	4.753-13	4.673-12	4.184-11
27	5.506-18	7.882-17	1.292-15	1.467-14	1.489-13	1.494-12	1.489-11
28	7.567-17	7.420-16	7.109-15	6.999-14	6.965-13	6.769-12	5.649-11
29	4.852-17	4.765-16	4.582-15	4.518-14	4.504-13	4.452-12	4.139-11
30	6.940-17	6.811-16	6.537-15	6.441-14	6.413-13	6.262-12	5.408-11
31	7.168-17	7.169-16	7.173-15	7.174-14	7.182-13	7.243-12	7.478-11
32	1.048-16	1.030-15	9.912-15	9.778-14	9.751-13	9.656-12	9.101-11
33	4.303-11	4.263-10	4.178-09	4.148-08	4.145-07	4.143-06	4.107-05
34	9.622-18	1.125-16	1.470-15	1.590-14	1.603-13	1.588-12	1.491-11
35	1.474-11	1.447-10	1.391-09	1.371-08	1.370-07	1.386-06	1.510-05
36	1.898-10	1.857-09	1.770-08	1.740-07	1.736-06	1.740-05	1.785-04
37	3.425-10	3.351-09	3.194-08	3.139-07	3.129-06	3.100-05	2.960-04
38	1.407-17	1.379-16	1.320-15	1.300-14	1.305-13	1.376-12	1.725-11
39	9.747-18	1.036-16	1.166-15	1.212-14	1.218-13	1.219-12	1.222-11
40	6.257-17	6.122-16	5.836-15	5.734-14	5.704-13	5.540-12	4.604-11
41	5.990-19	5.917-18	5.763-17	5.740-16	6.041-15	8.855-14	2.338-12
42	6.957-18	7.014-17	7.135-16	7.181-15	7.230-14	7.629-13	9.619-12
43	4.259-17	4.168-16	3.975-15	3.906-14	3.887-13	3.785-12	3.198-11
44	2.708-18	2.716-17	2.734-16	2.747-15	2.820-14	3.499-13	7.700-12
45	1.973-17	1.930-16	1.840-15	1.808-14	1.799-13	1.759-12	1.532-11
46	2.029-17	1.986-16	1.894-15	1.862-14	1.858-13	1.854-12	1.884-11

TABLE IIIB. Ni XXI Fractional Level Populations: With Proton Excitation

log(Den.)	8	9	10	11	12	13	14
Key				Population			
47	9.270-19	1.277-17	2.020-16	2.286-15	2.399-14	3.162-13	7.780-12
48	7.326-18	7.854-17	8.974-16	9.369-15	9.486-14	1.014-12	1.445-11
49	2.857-18	2.922-17	3.058-16	3.116-15	3.223-14	4.161-13	9.190-12
50	5.844-19	3.228-17	8.832-16	1.078-14	1.102-13	1.099-12	1.062-11
51	1.248-12	1.257-11	1.277-10	1.287-09	1.317-08	1.589-07	3.193-06
52	3.714-20	3.965-19	4.519-18	4.997-17	7.952-16	3.481-14	1.737-12
53	1.129-17	1.109-16	1.067-15	1.053-14	1.061-13	1.155-12	1.647-11
54	3.208-19	4.157-18	6.175-17	6.949-16	7.780-15	1.461-13	5.014-12
55	5.864-17	5.743-16	5.487-15	5.397-14	5.377-13	5.292-12	4.825-11
56	4.175-19	4.226-18	4.338-17	4.443-16	5.132-15	1.164-13	5.516-12
57	5.845-19	5.791-18	5.682-17	5.724-16	6.535-15	1.412-13	5.778-12
58	6.498-20	6.875-19	7.679-18	8.017-17	8.660-16	1.453-14	6.067-13

TABLE IVA. Ni XXI Line Intensities: Without Proton Excitation

log(Den.)			8	9	10	11	12	13	14
j	i	Wavelength				Intensity			
54	3	11.197	5.87-06	8.12-05	1.28-03	1.45-02	1.62-01	2.95+00	9.71+01
45	1	11.227	3.78-04	3.67-03	3.45-02	3.37-01	3.36+00	3.28+01	2.84+02
50	2	11.227	1.74-05	1.02-03	2.76-02	3.35-01	3.42+00	3.39+01	3.17+02
57	3	11.229	4.87-06	4.81-05	4.69-04	4.72-03	5.43-02	1.21+00	4.97+01
46	1	11.241	1.26-04	1.23-03	1.15-02	1.13-01	1.13+00	1.12+01	1.14+02
55	1	11.242	8.96-05	8.72-04	8.21-03	8.04-02	8.01-01	7.88+00	7.17+01
42	1	11.257	2.55-05	2.57-04	2.63-03	2.65-02	2.67-01	2.83+00	3.61+01
50	3	11.272	7.81-07	4.56-05	1.24-03	1.50-02	1.53-01	1.52+00	1.42+01
49	3	11.286	3.50-05	3.60-04	3.82-03	3.90-02	4.05-01	5.28+00	1.17+02
39	1	11.292	3.06-05	3.31-04	3.84-03	4.02-02	4.04-01	4.04+00	4.01+01
38	1	11.298	7.10-05	6.91-04	6.52-03	6.40-02	6.43-01	6.83+00	8.76+01
43	1	11.302	9.65-04	9.37-03	8.81-02	8.62-01	8.57+00	8.33+01	7.00+02
47	4	11.318	3.42-06	5.09-05	8.55-04	9.74-03	1.02-01	1.30+00	2.98+01
56	4	11.318	1.42-05	1.44-04	1.49-03	1.52-02	1.76-01	3.95+00	1.86+02
40	1	11.319	1.62-03	1.57-02	1.48-01	1.44+00	1.43+01	1.39+02	1.15+03
57	4	11.336	8.22-06	8.12-05	7.92-04	7.97-03	9.18-02	2.04+00	8.39+01
34	1	11.364	1.53-05	1.87-04	2.57-03	2.81-02	2.83-01	2.80+00	2.59+01
53	3	11.369	2.08-05	2.03-04	1.93-03	1.90-02	1.92-01	2.11+00	3.08+01
32	1	11.369	7.62-05	7.44-04	7.08-03	6.96-02	6.94-01	6.87+00	6.48+01
30	1	11.372	2.48-04	2.42-03	2.30-02	2.25-01	2.24+00	2.19+01	1.88+02
50	4	11.379	5.71-07	3.34-05	9.04-04	1.10-02	1.12-01	1.11+00	1.04+01
29	1	11.387	9.37-05	9.15-04	8.69-03	8.54-02	8.51-01	8.41+00	7.83+01
45	3	11.392	2.13-05	2.07-04	1.95-03	1.90-02	1.89-01	1.85+00	1.60+01
49	4	11.398	1.69-05	1.74-04	1.84-03	1.88-02	1.95-01	2.55+00	5.67+01
39	2	11.410	2.45-05	2.65-04	3.07-03	3.22-02	3.23-01	3.23+00	3.21+01
48	4	11.414	2.66-05	2.91-04	3.43-03	3.61-02	3.66-01	3.89+00	5.40+01
42	3	11.423	7.98-05	8.07-04	8.25-03	8.31-02	8.38-01	8.88+00	1.13+02
39	3	11.459	1.75-05	1.90-04	2.20-03	2.30-02	2.31-01	2.31+00	2.30+01
38	3	11.465	1.94-04	1.89-03	1.79-02	1.75-01	1.76+00	1.87+01	2.40+02
43	3	11.468	7.62-05	7.41-04	6.96-03	6.81-02	6.77-01	6.58+00	5.53+01
34	2	11.484	4.08-05	4.99-04	6.86-03	7.49-02	7.55-01	7.46+00	6.90+01
45	4	11.506	1.35-04	1.31-03	1.23-02	1.20-01	1.20+00	1.17+01	1.01+02
44	4	11.511	2.55-05	2.56-04	2.58-03	2.60-02	2.67-01	3.33+00	7.34+01
46	4	11.516	2.79-04	2.71-03	2.55-02	2.49-01	2.49+00	2.48+01	2.51+02
28	1	11.539	7.02-04	6.84-03	6.47-02	6.34-01	6.31+00	6.12+01	5.07+02
26	1	11.539	1.45-04	1.42-03	1.36-02	1.34-01	1.34+00	1.31+01	1.17+02
29	3	11.556	2.18-05	2.12-04	2.02-03	1.98-02	1.98-01	1.95+00	1.82+01
39	4	11.575	2.61-05	2.83-04	3.28-03	3.43-02	3.45-01	3.45+00	3.42+01
40	4	11.597	4.25-05	4.13-04	3.88-03	3.79-02	3.77-01	3.66+00	3.02+01
24	1	11.604	3.59-05	3.64-04	3.75-03	3.79-02	3.79-01	3.71+00	3.28+01
21	1	11.606	9.23-05	9.10-04	8.84-03	8.75-02	8.72-01	8.53+00	7.40+01
22	1	11.606	7.32-05	7.24-04	7.07-03	7.01-02	6.98-01	6.84+00	6.00+01
27	2	11.614	3.60-05	5.61-04	9.74-03	1.11-01	1.13+00	1.13+01	1.10+02
34	4	11.650	1.37-05	1.68-04	2.31-03	2.52-02	2.54-01	2.51+00	2.32+01
30	4	11.658	2.82-05	2.75-04	2.61-03	2.56-02	2.55-01	2.48+00	2.13+01
27	3	11.664	1.17-05	1.82-04	3.16-03	3.61-02	3.67-01	3.66+00	3.56+01

TABLE IVA. Ni XXI Line Intensities: Without Proton Excitation

log(Den.)			8	9	10	11	12	13	14
j	i	Wavelength				Intensity			
26	3	11.714	7.07-05	6.93-04	6.65-03	6.55-02	6.53-01	6.41+00	5.74+01
23	3	11.781	9.15-06	9.58-05	1.05-03	1.08-02	1.08-01	1.07+00	9.98+00
15	1	12.209	1.09-04	1.06-03	9.96-03	9.75-02	9.70-01	9.56+00	8.84+01
13	1	12.276	3.29-05	3.22-04	3.08-03	3.04-02	3.03-01	3.00+00	2.85+01
12	1	12.446	3.40-05	3.41-04	3.44-03	3.45-02	3.44-01	3.36+00	2.91+01
11	1	12.497	5.25-05	5.21-04	5.14-03	5.12-02	5.10-01	4.99+00	4.33+01
16	4	12.500	3.62-05	3.51-04	3.30-03	3.23-02	3.23-01	3.28+00	3.67+01
15	4	12.533	1.22-05	1.19-04	1.12-03	1.09-02	1.09-01	1.07+00	9.90+00
36	6	12.833	1.28-05	1.24-04	1.17-03	1.14-02	1.14-01	1.14+00	1.17+01
35	6	12.850	3.48-05	3.40-04	3.23-03	3.17-02	3.16-01	3.20+00	3.49+01
33	6	12.903	4.74-05	4.68-04	4.56-03	4.52-02	4.51-01	4.51+00	4.49+01
25	6	13.203	9.36-05	9.28-04	9.13-03	9.07-02	9.05-01	8.84+00	7.63+01
9	1	69.623	1.54-04	1.53-03	1.51-02	1.50-01	1.53+00	1.74+01	3.24+02
9	2	74.433	1.86-05	1.85-04	1.83-03	1.82-02	1.85-01	2.11+00	3.92+01
9	3	76.452	1.60-05	1.59-04	1.57-03	1.56-02	1.58-01	1.81+00	3.36+01
9	4	81.696	1.59-03	1.58-02	1.55-01	1.55+00	1.57+01	1.79+02	3.33+03
7	1	88.810	5.43-03	5.73-02	6.37-01	6.58+00	6.60+01	6.52+02	5.99+03
8	3	93.914	8.13-06	8.75-05	1.02-03	1.31-02	3.74-01	2.59+01	1.37+03
6	1	95.850	1.79-02	1.74-01	1.64+00	1.60+01	1.59+02	1.57+03	1.43+04
7	2	96.788	2.48-03	2.62-02	2.91-01	3.00+00	3.01+01	2.97+02	2.73+03
9	5	97.135	1.09-04	1.08-03	1.06-02	1.06-01	1.08+00	1.23+01	2.28+02
7	3	100.230	1.87-03	1.98-02	2.20-01	2.27+00	2.28+01	2.25+02	2.06+03
6	3	109.289	4.57-03	4.44-02	4.18-01	4.09+00	4.07+01	4.01+02	3.64+03
7	4	109.439	2.03-05	2.14-04	2.38-03	2.46-02	2.47-01	2.44+00	2.24+01
6	4	120.330	1.22-03	1.19-02	1.12-01	1.10+00	1.09+01	1.07+02	9.76+02
7	5	139.044	1.40-04	1.48-03	1.65-02	1.70-01	1.71+00	1.69+01	1.55+02
37	15	160.865	6.36-05	6.18-04	5.81-03	5.68-02	5.66-01	5.60+00	5.34+01
25	11	161.182	2.51-05	2.49-04	2.45-03	2.43-02	2.43-01	2.37+00	2.05+01
36	16	166.766	2.81-05	2.73-04	2.56-03	2.51-02	2.50-01	2.51+00	2.58+01
5	3	359.054	3.32-04	3.42-03	3.62-02	3.70-01	3.74+00	4.04+01	5.64+02
4	1	471.144	5.29-03	5.26-02	5.19-01	5.16+00	5.13+01	4.91+02	3.44+03
3	1	779.485	1.00-02	9.99-02	9.97-01	9.95+00	9.87+01	9.07+02	4.97+03
4	3	1191.047	1.31-04	1.30-03	1.28-02	1.28-01	1.27+00	1.21+01	8.52+01
3	2	2818.491	1.60-04	1.60-03	1.60-02	1.60-01	1.58+00	1.46+01	7.97+01

TABLE IVB. Ni XXI Line Intensities: With Proton Excitation

log(Den.)			8	9	10	11	12	13	14
j	i	Wavelength				Intensity			
54	3	11.197	5.78-06	7.49-05	1.11-03	1.25-02	1.40-01	2.63+00	9.03+01
45	1	11.227	3.79-04	3.70-03	3.53-02	3.47-01	3.45+00	3.37+01	2.94+02
50	2	11.227	1.41-05	7.81-04	2.14-02	2.61-01	2.66+00	2.66+01	2.57+02
57	3	11.229	4.87-06	4.83-05	4.73-04	4.77-03	5.45-02	1.18+00	4.82+01
46	1	11.241	1.27-04	1.24-03	1.18-02	1.16-01	1.16+00	1.16+01	1.18+02
55	1	11.242	8.97-05	8.79-04	8.39-03	8.26-02	8.23-01	8.10+00	7.38+01
42	1	11.257	2.54-05	2.57-04	2.61-03	2.63-02	2.64-01	2.79+00	3.52+01
50	3	11.272	6.34-07	3.50-05	9.57-04	1.17-02	1.19-01	1.19+00	1.15+01
49	3	11.286	3.49-05	3.57-04	3.74-03	3.81-02	3.94-01	5.09+00	1.12+02
39	1	11.292	3.05-05	3.24-04	3.65-03	3.79-02	3.81-01	3.82+00	3.82+01
38	1	11.298	7.10-05	6.96-04	6.66-03	6.56-02	6.59-01	6.95+00	8.71+01
43	1	11.302	9.66-04	9.45-03	9.01-02	8.86-01	8.81+00	8.58+01	7.25+02
47	4	11.318	3.35-06	4.62-05	7.31-04	8.27-03	8.68-02	1.14+00	2.82+01
56	4	11.318	1.41-05	1.43-04	1.47-03	1.51-02	1.74-01	3.94+00	1.87+02
40	1	11.319	1.62-03	1.58-02	1.51-01	1.48+00	1.48+01	1.43+02	1.19+03
57	4	11.336	8.22-06	8.15-05	7.99-04	8.05-03	9.19-02	1.99+00	8.13+01
34	1	11.364	1.52-05	1.77-04	2.32-03	2.51-02	2.53-01	2.50+00	2.35+01
53	3	11.369	2.08-05	2.05-04	1.97-03	1.94-02	1.96-01	2.13+00	3.04+01
32	1	11.369	7.62-05	7.49-04	7.21-03	7.11-02	7.09-01	7.03+00	6.62+01
30	1	11.372	2.49-04	2.44-03	2.34-02	2.31-01	2.30+00	2.24+01	1.94+02
29	1	11.387	9.38-05	9.21-04	8.86-03	8.73-02	8.71-01	8.61+00	8.00+01
45	3	11.392	2.14-05	2.09-04	1.99-03	1.96-02	1.95-01	1.90+00	1.66+01
49	4	11.398	1.69-05	1.73-04	1.81-03	1.84-02	1.90-01	2.46+00	5.43+01
39	2	11.410	2.44-05	2.60-04	2.92-03	3.04-02	3.05-01	3.06+00	3.06+01
48	4	11.414	2.65-05	2.84-04	3.25-03	3.39-02	3.43-01	3.67+00	5.23+01
42	3	11.423	7.98-05	8.05-04	8.18-03	8.24-02	8.29-01	8.75+00	1.10+02
39	3	11.459	1.75-05	1.86-04	2.09-03	2.17-02	2.18-01	2.19+00	2.19+01
38	3	11.465	1.95-04	1.91-03	1.83-02	1.80-01	1.81+00	1.90+01	2.39+02
43	3	11.468	7.63-05	7.47-04	7.12-03	7.00-02	6.97-01	6.78+00	5.73+01
34	2	11.484	4.05-05	4.73-04	6.19-03	6.69-02	6.75-01	6.68+00	6.27+01
45	4	11.506	1.35-04	1.32-03	1.26-02	1.24-01	1.23+00	1.20+01	1.05+02
44	4	11.511	2.55-05	2.56-04	2.58-03	2.59-02	2.66-01	3.30+00	7.26+01
46	4	11.516	2.79-04	2.73-03	2.61-02	2.56-01	2.56+00	2.55+01	2.59+02
28	1	11.539	7.03-04	6.89-03	6.60-02	6.50-01	6.47+00	6.29+01	5.25+02
26	1	11.539	1.45-04	1.43-03	1.38-02	1.37-01	1.36+00	1.34+01	1.20+02
29	3	11.556	2.18-05	2.14-04	2.06-03	2.03-02	2.02-01	2.00+00	1.86+01
39	4	11.575	2.60-05	2.77-04	3.12-03	3.24-02	3.25-01	3.26+00	3.26+01
40	4	11.597	4.26-05	4.16-04	3.97-03	3.90-02	3.88-01	3.77+00	3.13+01
24	1	11.604	3.59-05	3.63-04	3.71-03	3.74-02	3.74-01	3.67+00	3.25+01
21	1	11.606	9.24-05	9.14-04	8.94-03	8.86-02	8.83-01	8.65+00	7.53+01
22	1	11.606	7.32-05	7.26-04	7.13-03	7.08-02	7.06-01	6.92+00	6.09+01
27	2	11.614	3.52-05	5.04-04	8.26-03	9.38-02	9.52-01	9.56+00	9.52+01
34	4	11.650	1.36-05	1.59-04	2.08-03	2.25-02	2.27-01	2.25+00	2.11+01
30	4	11.658	2.82-05	2.77-04	2.66-03	2.62-02	2.61-01	2.55+00	2.20+01
27	3	11.664	1.14-05	1.63-04	2.68-03	3.04-02	3.09-01	3.10+00	3.08+01
26	3	11.714	7.07-05	6.97-04	6.75-03	6.67-02	6.65-01	6.54+00	5.85+01

TABLE IVB. Ni XXI Line Intensities: With Proton Excitation

log(Den.)			8	9	10	11	12	13	14
j	i	Wavelength				Intensity			
23	3	11.781	9.13-06	9.46-05	1.02-03	1.04-02	1.04-01	1.03+00	9.66+00
15	1	12.209	1.09-04	1.07-03	1.02-02	1.00-01	9.98-01	9.84+00	9.12+01
13	1	12.276	3.29-05	3.24-04	3.13-03	3.10-02	3.09-01	3.06+00	2.90+01
12	1	12.446	3.40-05	3.41-04	3.43-03	3.44-02	3.43-01	3.35+00	2.91+01
11	1	12.497	5.25-05	5.22-04	5.17-03	5.15-02	5.13-01	5.03+00	4.38+01
16	4	12.500	3.62-05	3.54-04	3.38-03	3.32-02	3.32-01	3.37+00	3.76+01
15	4	12.533	1.22-05	1.20-04	1.14-03	1.12-02	1.12-01	1.10+00	1.02+01
36	6	12.833	1.28-05	1.25-04	1.19-03	1.17-02	1.17-01	1.17+00	1.21+01
35	6	12.850	3.48-05	3.42-04	3.29-03	3.24-02	3.24-01	3.28+00	3.57+01
33	6	12.903	4.74-05	4.69-04	4.60-03	4.57-02	4.56-01	4.56+00	4.52+01
25	6	13.203	9.36-05	9.31-04	9.18-03	9.14-02	9.11-01	8.91+00	7.73+01
9	1	69.623	1.54-04	1.53-03	1.52-02	1.51-01	1.54+00	1.76+01	3.27+02
9	2	74.433	1.87-05	1.86-04	1.84-03	1.83-02	1.86-01	2.12+00	3.95+01
9	3	76.452	1.60-05	1.59-04	1.57-03	1.57-02	1.59-01	1.82+00	3.39+01
9	4	81.696	1.59-03	1.58-02	1.56-01	1.56+00	1.58+01	1.81+02	3.36+03
7	1	88.810	5.41-03	5.65-02	6.14-01	6.31+00	6.33+01	6.25+02	5.77+03
8	3	93.914	8.11-06	8.58-05	9.76-04	1.23-02	3.46-01	2.38+01	1.29+03
6	1	95.850	1.79-02	1.75-01	1.67+00	1.64+01	1.64+02	1.61+03	1.47+04
7	2	96.788	2.47-03	2.58-02	2.80-01	2.88+00	2.89+01	2.85+02	2.63+03
9	5	97.135	1.09-04	1.08-03	1.07-02	1.07-01	1.08+00	1.24+01	2.30+02
7	3	100.230	1.87-03	1.95-02	2.12-01	2.18+00	2.18+01	2.16+02	1.99+03
6	3	109.289	4.57-03	4.48-02	4.27-01	4.20+00	4.19+01	4.12+02	3.74+03
7	4	109.439	2.02-05	2.11-04	2.29-03	2.36-02	2.36-01	2.34+00	2.16+01
6	4	120.330	1.22-03	1.20-02	1.14-01	1.13+00	1.12+01	1.10+02	1.00+03
7	5	139.044	1.40-04	1.46-03	1.59-02	1.63-01	1.64+00	1.62+01	1.49+02
37	15	160.865	6.37-05	6.23-04	5.94-03	5.84-02	5.82-01	5.77+00	5.51+01
25	11	161.182	2.51-05	2.50-04	2.46-03	2.45-02	2.45-01	2.39+00	2.07+01
36	16	166.766	2.81-05	2.75-04	2.62-03	2.58-02	2.57-01	2.58+00	2.65+01
5	3	359.054	3.31-04	3.39-03	3.55-02	3.61-01	3.65+00	3.95+01	5.55+02
4	1	471.144	5.29-03	5.27-02	5.21-01	5.19+00	5.16+01	4.94+02	3.46+03
3	1	779.485	9.04-03	9.06-02	9.08-01	9.08+00	9.01+01	8.32+02	4.65+03
4	3	1191.047	1.31-04	1.30-03	1.29-02	1.28-01	1.28+00	1.22+01	8.57+01
3	2	2818.491	1.45-04	1.45-03	1.46-02	1.46-01	1.45+00	1.33+01	7.46+01

Figure Captions

Figure 1. Application of the Burgess and Tully (1992) scaling laws to collision strengths and effective collision strengths for an optically allowed transition. **Upper left**: Collision strengths as a function of the incident energy; **Upper right**: scaled collision strengths as a function of scaled energy: the values at $E_{scal}=0$ is extrapolated from the available data; **Lower left**: effective collision strengths as a function of electron temperature; **Lower right**: scaled effective collision strengths as a function of scaled temperature: the dashed line indicates the interpolated data.

Figure 2. Same as Figure 1 for a forbidden transition. $E_{scal}=1$ is also extrapolated from the available data.

Figure 3. Same as Figure 1 for an intercombination transition. $E_{scal}=1$ is also extrapolated from the available data.

Ni XXI 2s22p4 3P2.0 - 2p3.(2D*).3s 3D2.0 (1:13) type=1 type_ups=1 c=2.0 c_ups=3.0

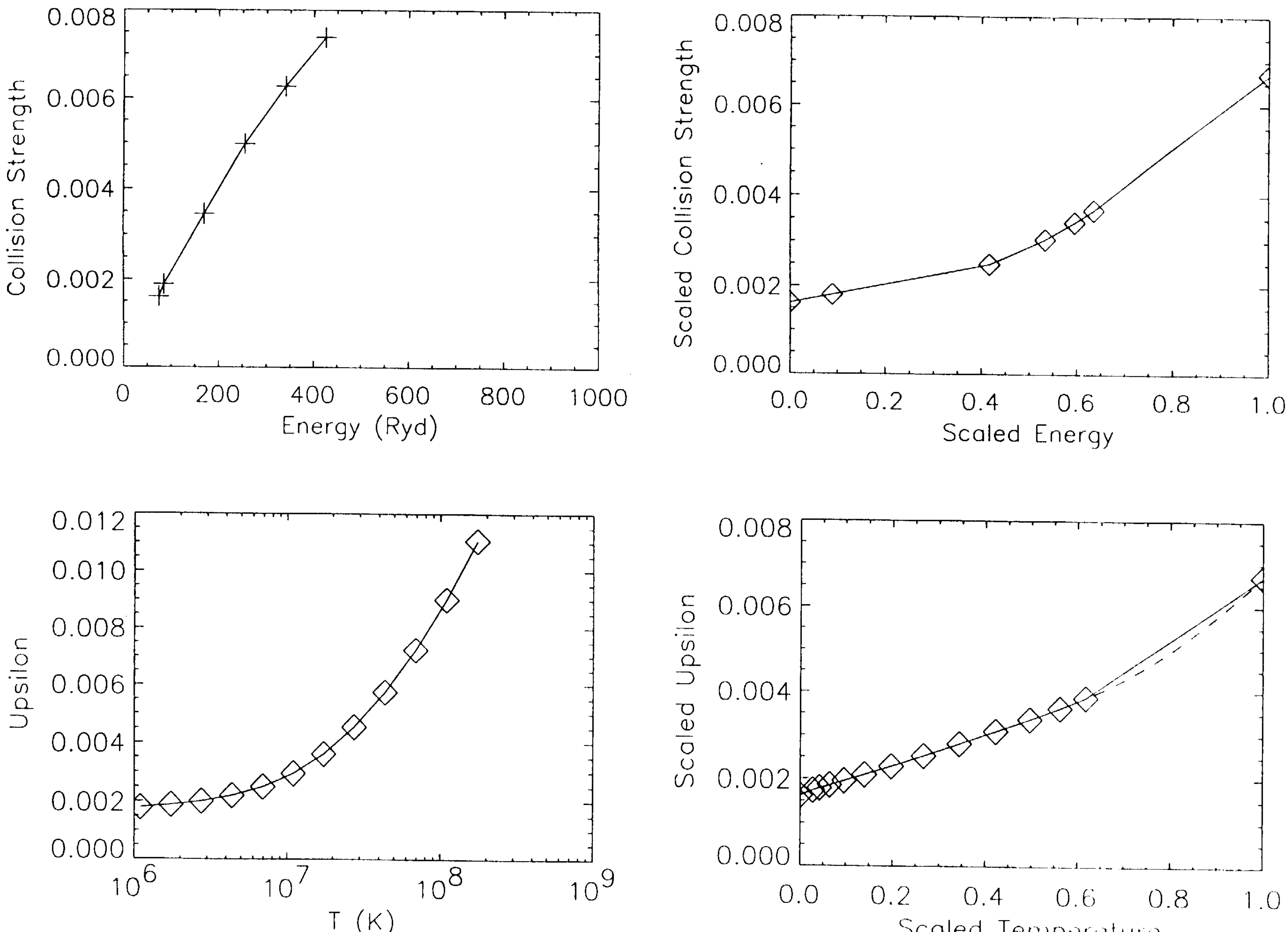

ni_21.omdat% Collision strengths:% Oscillator strengths:%% E. Landi 2001

Ni XXI 2s22p4 3P2.0 - 2p3.(2D*).3d 3G4.0 (1:36) type=2 type_ups=2 c=1./ c_ups=1.1

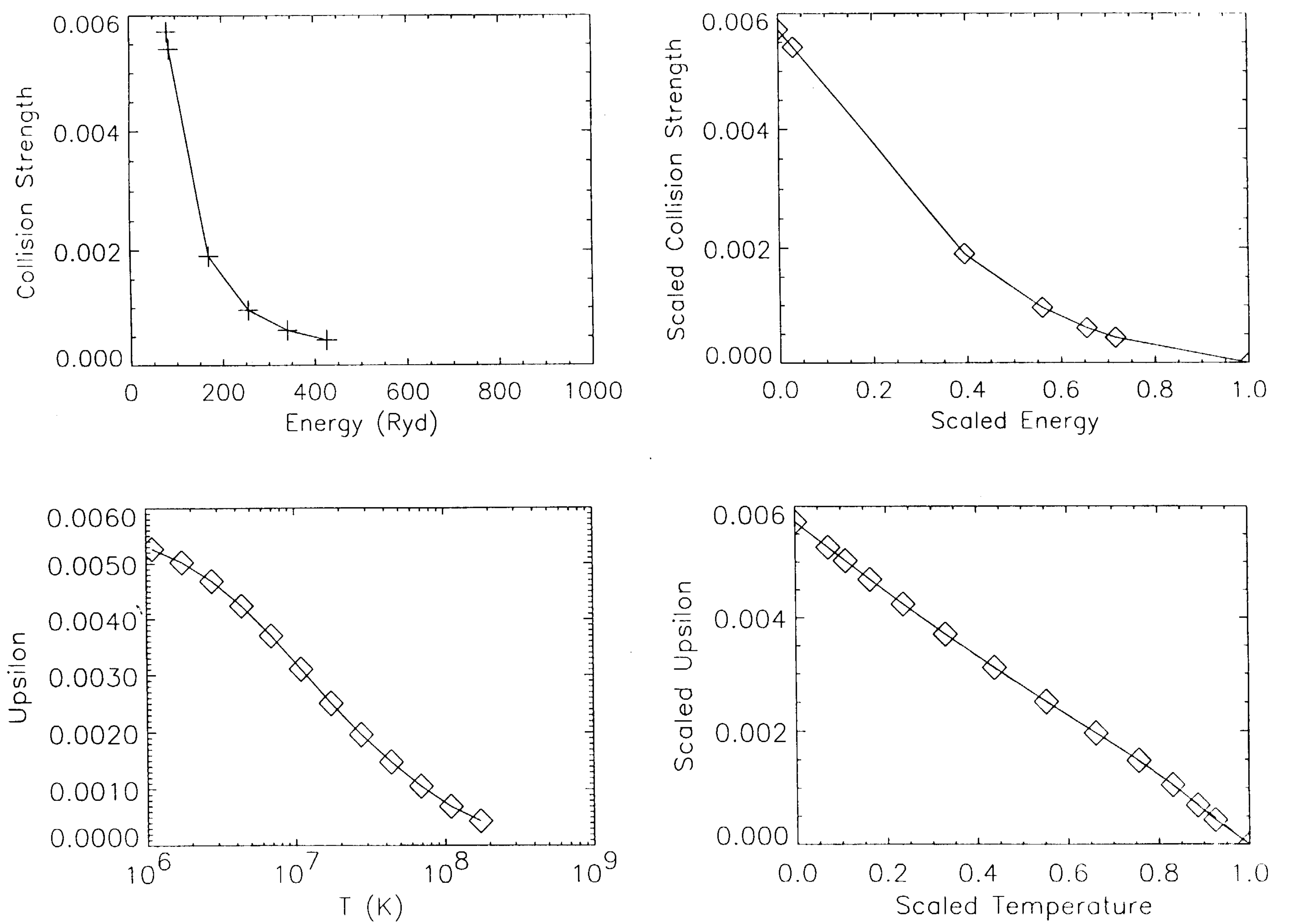

ni_21.omdat% Collision strengths:% Oscillator strengths:%% E. Landi 2001

Ni XXI 2s22p4 3P2.0 - 2p3.(2D*).3d 1S0.0 (1:31) type=3 type_ups=3 c=1.5 c_ups=1.4

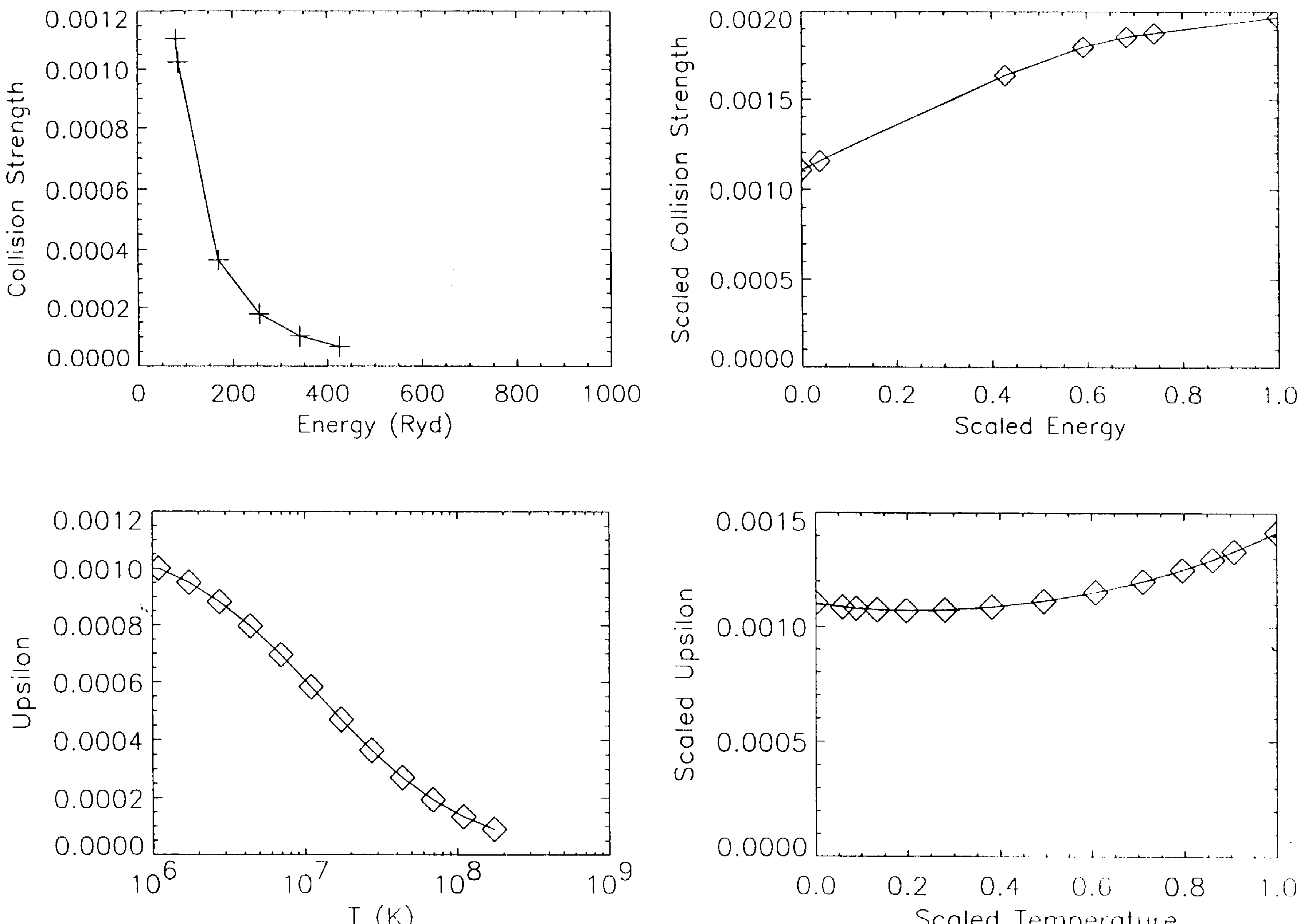

ni_21.omdat% Collision strengths:% Oscillator strengths:%% E. Landi 2001